Biophysical Journal Volume 69 August 1995 323–328

Real Time Imaging of Single Fluorophores on Moving Actin with an Epifluorescence Microscope

Ichiro Sase,* Hidetake Miyata,* John E. T. Corrie,‡ James S. Craik,‡ and Kazuhiko Kinosita, Jr.*

*Department of Physics, Faculty of Science and Technology, Keio University, Hiyoshi 3-14-1, Kohoku-ku, Yokohama 223, Japan; and ‡National Institute for Medical Research, The Ridgeway, Mill Hill, London NW7 1AA, United Kingdom

ABSTRACT Relatively simple modifications of an ordinary epifluorescence microscope have greatly reduced its background luminescence, allowing continuous and real time imaging of single fluorophores in an aqueous medium. Main modifications were changing the excitation light path and setting an aperture stop so that stray light does not scatter inside the microscope. A simple and accurate method using actin filaments is presented to establish the singularity of the observed fluorophores. It was possible, at the video rate of 30 frames/s, to image individual tetramethylrhodamine fluorophores bound to actin filaments sliding over heavy meromyosin. The successful imaging of moving fluorophores demonstrates that conventional microscopes may become a routine tool for studying dynamic interactions among individual biomolecules in physiological environments.

INTRODUCTION

Continuous imaging of individual molecules at work in living systems offers great promise for understanding biological mechanisms, where interactions among individual molecules are crucial. Previous landmarks toward this goal include fluorescence imaging of single molecules of antibody (Hirschfeld et al., 1976), DNA (Morikawa and Yanagida, 1981), and a cell surface receptor (Barak and Webb, 1981). In these cases, the target macromolecule could be decorated with many ($\sim 10^2$) fluorophores. However, multiple labeling often seriously affects molecular functions. Thus, the next step would be single fluorophore imaging, which would allow visualization of a host of biological interactions involving proteins and ligands. Detection, although not imaging, of individual fluorophores was reported in 1990 (Shera et al., 1990), which demonstrated that sufficient photons can be collected from a single chromophore to indicate its presence. In significant recent work, individual dye molecules immobilized in a dry or solid environment have been imaged (Betzig and Chichester, 1993; Ambrose et al., 1994; Ishikawa et al., 1994; Güttler et al., 1994). However, none of these achievements is directly appropriate for biological applications, where experiments must be conducted in an aqueous medium.

Elimination of background light is the key to successful imaging of a single fluorophore. An intense excitation light produces unwanted emission from virtually everything in the excitation path, including microscope components themselves. The previous successes (Betzig and Chichester, 1993; Ambrose et al., 1994; Ishikawa et al., 1994; Güttler et al., 1994) were based on minimizing the overlap of excitation and detection paths or the excitation volume in the sample. Thus, a conventional epifluorescence microscope in which the excitation and detection paths overlap considerably is probably the least suitable optical system for the present purpose. Nevertheless, we chose to work on this system to be able to exploit all existing and future technology of conventional microscopes and associated systems.

Here we report on continuous imaging of individual fluorophores moving in an aqueous medium, which is the biological environment, but one where fluorophores bleach readily. The success might be considered an unexpected one in that the imaging was made with an ordinary epifluorescence microscope. The conventional microscope, already a powerful tool in biology, has acquired another role as a single-molecule imager.

MATERIALS AND METHODS

Optics

An inverted epifluorescence microscope (Diaphot TMD, Nikon, Tokyo, Japan) was used. The holder for an epifluorescence cassette was modified such that the excitation beam entered from the right-hand side and its unreflected portion exited on the left (Fig. 1). The concave lens in the objective turret was replaced with a quartz substitute (Sigma Koki, Saitama, Japan). Excitation source was a frequency-doubled Nd/YAG laser coupled to a single-mode optical fiber (model DPY425II-FP, Adlas, Lübeck, Germany). The fiber output (532 nm, 180 mW) was focused onto a rotating diffuser disk (lemon-skin filter), passed through a quarter-wave plate to eliminate polarization and a bandpass filter (not shown) to eliminate infrared components, and introduced into the microscope through external aperture and field diaphragms. A quartz dichroic mirror with a separation wavelength of 565 nm (Sigma Koki) deflected the beam toward a water immersion objective (63×, NA1.2, Carl Zeiss, Tokyo, Japan). Fluorescence was detected through a bandpass filter (transmission at 562–618 nm, Chroma Technology, Brattleboro, VT) with an image intensifier (model KS1381, Video Scope International, Washington D.C.) coupled to a CCD camera (model CCD-72, Dage-MTI, Michigan City, IN). Images were recorded on a Hi8 (model EVO-9650, Sony, Tokyo, Japan) video

---

Received for publication 6 March 1995 and in final form 5 May 1995.

Address reprint requests to Kazuhiko Kinosita, Department of Physics, Faculty of Science and Technology, Hiyoshi 3-14-1, Kohoku-ku, Yokohama 223, Japan. Tel.: 81-45-563-1141 (ext. 3975); Fax: 81-45-563-1761.

Abbreviations used: TMR, tetramethylrhodamine; MOPS, 3-morpholinopropanesulfonic acid; Tris, 2-amino-2-hydroxymethyl-1,3-propanediol.

© 1995 by the Biophysical Society

0006-3495/95/08/323/06 $2.00

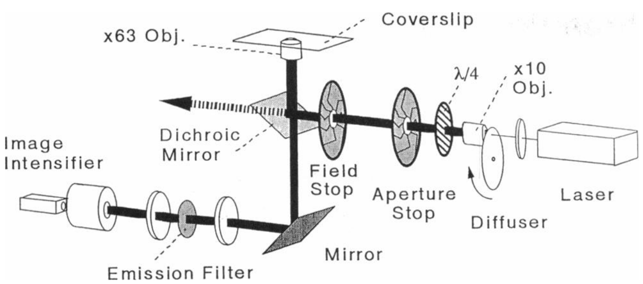

FIGURE 1 Diagram of the optical system for single fluorophore imaging (see Materials and Methods for details). The excitation beam from the laser enters the microscope from the right-hand side, and its unreflected portion exits on the left. The aperture diaphragm limits the beam width at the objective.

recorder, or directly on a digital image processor (model C2000, Hamamatsu Photonics, Shizuoka, Japan) used for image analysis.

Preparation of 5-iodoacetamido-tetramethylrhodamine-labeled actin

50 μM of pure 5-iodoacetamido-tetramethylrhodamine (TMR) (synthesized as described in Corrie and Craik, 1994), and 10 μM of rabbit skeletal actin in F-buffer (0.1 M KCl, 2 mM MOPS, 1 mM $MgCl_2$, 1.5 mM NaN_3, 0.1 mM ATP, pH 7.0) were mixed and incubated at 0°C for 15 h. The reaction mixture was dialyzed against G-buffer (2 mM Tris, 0.2 mM $CaCl_2$, 0.3 mM NaN_3, 0.2 mM ATP, pH 8.0) and centrifuged at 346,000 × g for 1 h. The supernatant was polymerized in F-buffer, and the resultant F-actin was collected by centrifugation. After several cycles of polymerization/depolymerization, the final product in G-buffer was passed through a Sephadex G-25 column. 40% of actin was labeled, as estimated from $\epsilon_{\sim 550\mathrm{nm}} = 96{,}900\ \mathrm{M^{-1}\ cm^{-1}}$ (Corrie and Craik, 1994) and $\epsilon_{290\mathrm{nm}} = 20{,}150\ \mathrm{M^{-1}\ cm^{-1}}$ (J. E. T. Corrie and J. S. Craik, unpublished data) for TMR and $\epsilon_{290\mathrm{nm}} = 0.63\ \mathrm{mg^{-1}\ ml\ cm^{-1}}$ for monomeric actin (Houk and Ue, 1974). The labeled actin was mixed with unlabeled actin at various ratios (total actin concentration of 5 or 25 μM) and polymerized in F-buffer at 0°C for 48 h in the presence of 10× molar excess of phalloidin. More than 99% of labeled actin sedimented by centrifugation at 346,000 × g for 1 h, showing that the TMR content in filaments was the same as in the filament-forming mixture. For imaging, the actin filaments were diluted in F-buffer (deoxygenated by bubbling N_2 gas) and introduced in between a pair of quartz coverslips cleaned with KOH. The coverslip closer to the objective was precoated with polylysine to bind actin filaments.

Motility assay

Motility measurement of F-actin over the heavy meromyosin was done as described (Miyata et al., 1994, 1995) except for the following. The quartz coverslip was pretreated with polylysine (Ohichi et al., 1993) instead of nitrocellulose. Enzymatic deoxygenation was not adopted, but the assay buffer was bubbled with N_2 gas immediately before use. Heavy meromyosin was applied at 80 μg ml^{-1}, and [ATP] was 2 mM. Images were recorded on a videotape and analyzed with the image processor.

RESULTS AND DISCUSSION

With several commercial microscopes tested, the level of background light was more than an order of magnitude higher than the intensity expected from a single fluorophore. This high background could be reduced by two orders of magnitude by two simple means (see Fig. 1). 1) The small fraction of excitation beam that unavoidably passed through the dichroic mirror for epi-illumination was let out of the microscope, which prevented it from being scattered in the microscope body. 2) The excitation beam was narrowed at the position of the objective such that the beam passed cleanly through the center of the objective without hitting its bottom diaphragm or the lens rims. Laser excitation, adopted for the purpose of intense monochromatic excitation, helped realize, but was not essential for, the above two points. Further reduction of background luminescence was achieved by the cumulative effects of 3) the use of a water-, not oil-, immersion objective, 4) individual selection of the objective, dichroic mirror, and filters, 5) the use of quartz instead of glass for coverslips and the concave lens in the turret, 6) appropriate positioning of the emission filter, and 7) careful cleaning of coverslips.

The cumulative background reduction allowed real time imaging of single molecules of tetramethylrhodamine, which is a widely used fluorescent probe. As a model system, we used actin labeled with 5-iodoacetamido-TMR (Corrie and Craik, 1994) for the following three reasons. 1) A single actin filament is easily visualized by labeling with TMR (Yanagida et al., 1984), and 1 μm of the filament is known to contain ~366 actin monomers (Egelman, 1985). 2) Actin has a single binding site for iodoacetamido-TMR (Tait and Frieden, 1982). These two points imply that a filament of TMR-actin constitutes a well defined intensity standard for comparison with a single TMR. Point 2 also ensures that individual dye molecules in the assembled filament are held apart and cannot self-quench. Finally, 3) an actin filament will slide steadily over a myosin-coated surface (Kron and Spudich, 1986; Kinosita et al., 1991; Miyata et al., 1994, 1995). Thus, by comparing successive video frames, the moving single fluorophores can be discriminated from nonmobile background noise.

We made a series of filament preparations containing different proportions of labeled actin. Fig. 2 shows images

FIGURE 2 (*A–E*) Fluorescence images of actin filaments with various TMR-actin contents. *N* represents the average number of TMR-actin per μm of filament, calculated as the fraction of labeled actin times 366 actin monomers/μm. Unlabeled actin was imaged in *E*, where an occasional impurity spot is shown. Bar, 10 μm. The filaments were in F-buffer (0.1 M KCl, 2 mM MOPS, 1 mM $MgCl_2$, 1.5 mM NaN_3, 0.1 mM ATP, pH 7.0) and bound to a polylysine-coated coverslip. Excitation intensities were 0.14 (*A*), 0.33 (*B*), 2.8 (*C*), and 11 (*D*, *E*) mW over an illuminated area of ~35-μm diameter. All images (integrations over 16 video frames, i.e., 0.53 s) were obtained at the same detector sensitivity and are reproduced here with same brightness level. (*F*) Reconstruction of a filament image from *D*. Image *D* was displaced in steps of 1/366 μm, and the resultant images were superimposed 1378 times (total displacement 3.8 μm). To compare with image *A*, the final image was divided by 11/0.14 (difference in excitation intensity) and multiplied by 150(*N* for image *A*)/366. (*G*, *H*) Images *A* and *F* presented in linearly color-coded intensity.

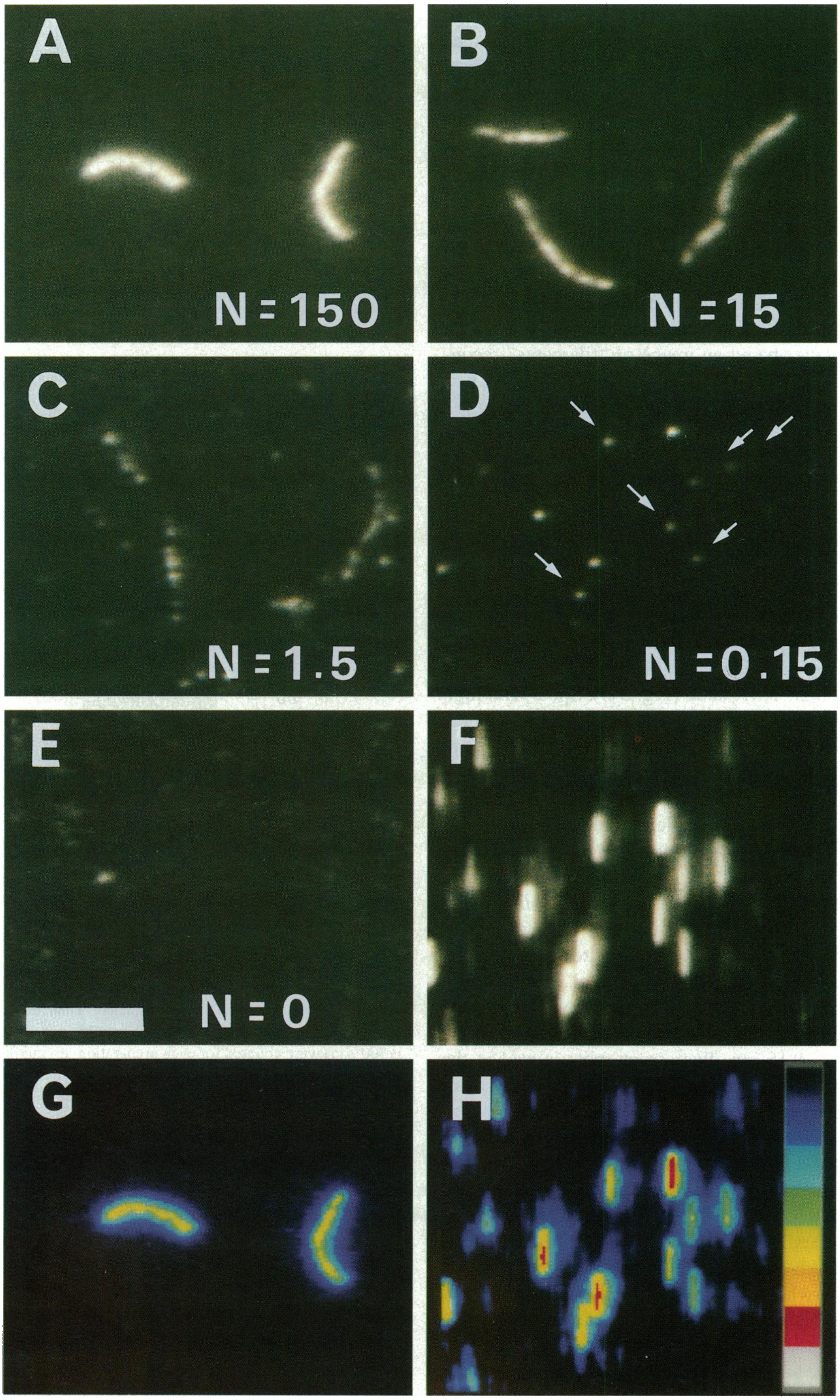
A
N = 150
B
N = 15
C
N = 1.5
D
N = 0.15
E
N = 0
F
G
H

of the filaments bound to a coverslip. As *N* (the average number of TMR/μm of filament) decreased, the appearance of the uniformly fluorescent filaments (Fig. 2 *A*) changed into a collection of dots in Fig. 2 *D*, as expected. In the range where filaments could be identified (Fig. 2 *A–C*), the fluorescence intensity of a filament with length *L* was proportional to *NL*, the number of fluorophores expected in that filament (see Fig. 3 *A*, where the intensity/*NL* is plotted). This shows that the fluorescence intensity was a reliable measure of the number of TMR-actin molecules. On this basis, we claim that fluorescent spots indicated with an arrow in Fig. 2 *D* represent single TMR fluorophores.

Justification of this claim comes from comparison of Fig. 2, *A* and *F*, the latter being an image of "filaments" reconstructed from the spots of Fig. 2 *D*. The reconstruction was made with the number of spots/1 μm of filament in Fig. 2 *F* equal to *N* in Fig. 2 *A* (150/μm). Thus, if a spot in Fig. 2 *D* represents a single TMR group, the corresponding "filament" in Fig. 2 *F* should have the same intensity as in Fig. 2 *A*. As seen in the pseudo-color representation in Fig. 2, *G* and *H*, the spots marked in Fig. 2 *D* approximately satisfy this criterion. Brighter spots in Fig. 2 *D* presumably represent two TMR fluorophores.

Fig. 3 *B* shows the distribution of spot intensities for the sample with the lowest *N* of 0.15/μm (Fig. 2 *D*). The peak of the distribution coincides with the arrow, the intensity expected for a single TMR-actin (Fig. 3 *A*). Spots with high intensities presumably represent closely apposed fluorophores. The majority of spots, however, should represent single fluorophores.

To demonstrate that the spots were not impurities but genuinely represented TMR-actin, we let the filaments slide over heavy meromyosin bound to the surface of a polylysine-coated coverslip. Bright filaments with $N = 150/\mu m$ ran at an average speed of 1.5 μm/s (Fig. 4 *A*). The filaments in this sample were shorter and the speed was lower compared with our standard motility assay in which the coverglass is pretreated with nitrocellulose (Kinosita et al., 1991; Miyata et al., 1994, 1995), because in the present study we had to use polylysine instead of nitrocellulose, which turned out to be fluorescent. For the sample with $N = 0.15/\mu m$, fluorescent spots moved at the same speed as the fluorescent filaments (Fig. 4, *B* and *C*). Most of the spots moved independently, which indicated that they were carried by different filaments as expected from the short filament lengths in this motility assay (Fig. 4 *A*). Occasionally, however, we found two spots moving in tandem (not shown). Fig. 4 *B* indicates that most of recognizable spots moved in the presence of ATP and, therefore, were TMR-actin (some photobleached during the observation interval).

Fig. 4 *C* shows whole traces of three spots. All three spots eventually photobleached abruptly at the arrowhead, a behavior expected for a single fluorophore. In this motile system, it could be argued that the filament carrying the spot might have dissociated from heavy meromyosin and floated out of focus. However, similar abrupt disappearance was recorded many times in the stationary system of Fig. 2 *D*. Because of incomplete deoxygenation, the average lifetime of fluorescent spots under the highest laser intensity (11 mW) was 2–3 s, but a considerable portion survived beyond 10 s as in Fig. 4 *C*. The apparent intensity fluctuation in Fig. 4 *C* is due in part to the relatively short integration time for each image (0.27 s) and in part to a high background fluorescence in the motility chamber into which solutions

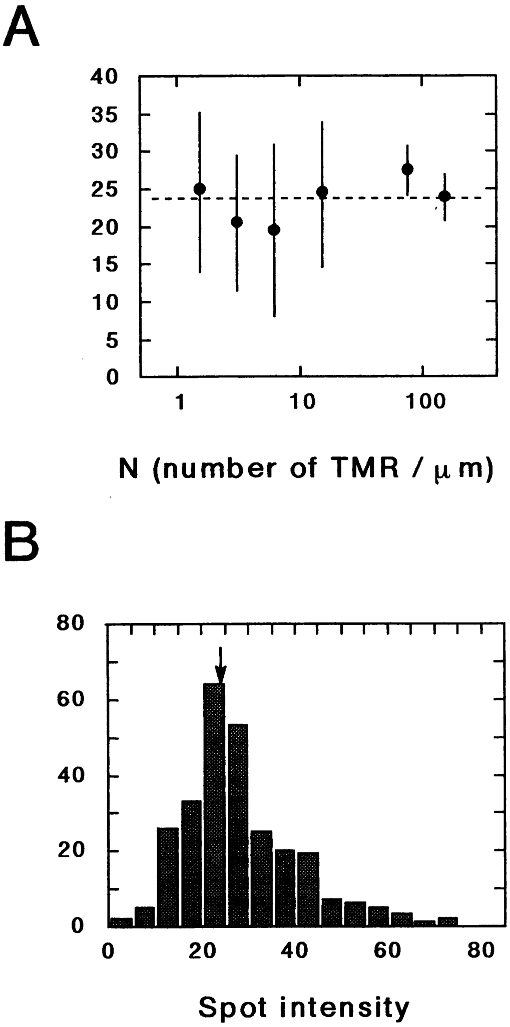

FIGURE 3 Fluorescence intensities of TMR in actin filaments. (*A*) Intensity (arbitrary unit) per single TMR estimated from filament images as in Fig. 2 *A–C*. Abscissa, *N*, is the average number of TMR per μm of filament for each preparation. To obtain the ordinate values, each filament in an image was enclosed in a rectangle and the fluorescence intensity was integrated over the entire rectangle. Background intensity, estimated in a nearby filament-free area, was subtracted. Then the integrated intensity was divided by $N \times L$ (L = filament length). ~20 filaments (total length ~300 μm) were counted for each preparation, giving the average intensity and SD (bar) in the plot. (*B*) Distribution of isolated spot intensities at $N = 0.15/\mu m$ (Fig. 2 *D*). The spot intensity is defined as the total intensity over a square 3.5 μm × 3.5 μm (15 × 15 pixels) enclosing the spot, corrected for a background near the spot. Where two spots were apposed within 2 μm, the aggregate intensity for two squares was divided in proportion to the peak intensities. Spots closer than 0.5 μm were not separated and counted as one. (Single spots had a diameter at e^{-1} times the peak intensity of ~0.7μ m.) The arrow indicates the intensity value for a single TMR estimated in *A*. For spots at this intensity, the brightest pixel in the spot had an uncorrected intensity 4 times the pixel intensity for background.

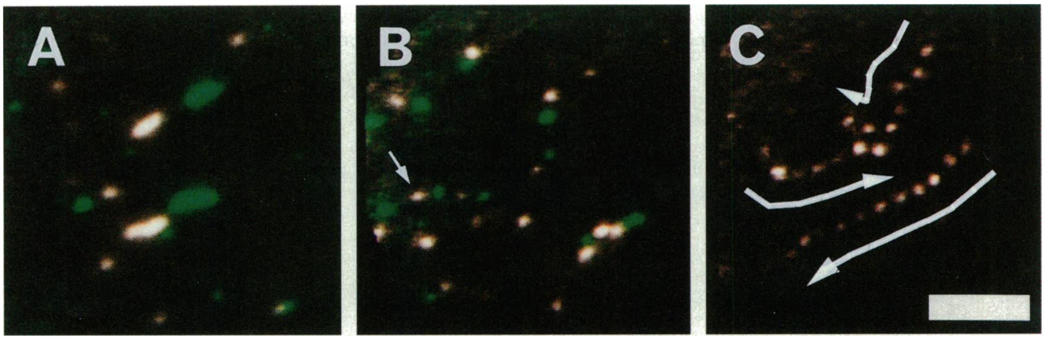

FIGURE 4 TMR-actin sliding over heavy meromyosin at 25°C. (*A*) Filaments with $N = 150/\mu\text{m}$. Two images at an interval of 2.5 s are superimposed, the second one shown in green. (*B*, *C*) Filaments with $N = 0.15/\mu\text{m}$. In *B*, green and white images were taken at 0.8-s interval. White spots unaccompanied with a green spot disappeared during the 0.8-s interval. The white spot with an arrow had an intensity expected for a single TMR. *C* is the superposition of sequential images at 1.1-s intervals, showing movements of three spots. Arrows indicate the direction of sliding. Bar, 10 μm. All images in *A*–*C* were integrated over eight video frames (0.27 s). Excitation intensity was 0.14 mW for *A* and 11 mW for *B* and *C*. All images are reproduced with the same brightness level.

had been infused several times. The peak intensity of these spots was, on average, twice the background intensity, compared with 4 to 1 in Fig. 2 *D*. Although fluctuation was larger in raw images without integration, spots could be located unambiguously in ~90% of images. In a more clean chamber as in Fig. 2 *D*, the intensity fluctuation was ~30% (SD) at the full video rate of 30 frames/s.

We conclude that we have been able to image, continuously for many seconds at the video rate of 30 frames/s, individual TMR fluorophores moving in an aqueous environment. Further reduction in background luminescence and more complete deoxygenation, both in progress at present, will improve the image quality and allow, for example, continuous observation of the orientation of a single molecule via polarization imaging (Kinosita et al., 1991; Suzuki et al., 1995).

As a final remark, we note that most of our efforts at single fluorophore imaging would have been realized better and more easily by microscope manufacturers. Thus, we believe the day will come soon when imaging "live" molecules becomes a routine task. The next challenge will be single fluorophore imaging in live cells, where one has to circumvent autofluorescence of the cells.

We thank Dr. D. R. Trentham (National Institute for Medical Research, Mill Hill, London, U.K.), who initiated our collaboration. Dye oligomers prepared by Drs. G. Marriott (Max Planck Institut für Biochemie, München, Germany), S. Maki, S. Nishiyama, and S. Yamamura (Keio University, Yokohama, Japan) were the key to our initial success.

This work was supported by a Fellowship of the Japan Society for the Promotion of Science for Japanese Junior Scientists, by Grants-in-Aid from the Ministry of Education, Science and Culture of Japan, and by Special Coordination Funds for Promoting Science and Technology from the Agency of Science and Technology of Japan.

Note added in proof—Recently, Funatsu et al. (1995) have also succeeded in imaging single fluorophores in an aqueous environment. Individual turnovers of myosin ATPase reaction have been visualized with total internal reflection fluorescence microscopy.

REFERENCES

Ambrose, W. P., P. M. Goodwin, J. C. Martin, and R. A. Keller. 1994. Single molecule detection and photochemistry on a surface using near-field optical excitation. *Phys. Rev. Lett.* 72:160–163.

Barak, L. S., and W. W. Webb. 1981. Fluorescent low density lipoprotein for observation of dynamics of individual receptor complexes on cultured human fibroblasts. *J. Cell Biol.* 90:595–604.

Betzig, E., and R. J. Chichester. 1993. Single molecules observed by near-field scanning optical microscopy. *Science.* 262:1422–1425.

Corrie, J. E. T., and J. S. Craik. 1994. Synthesis and characterisation of pure isomers of iodoacetamidotetramethylrhodamine. *J. Chem. Soc., Perkin Trans. 1*:2967–2974.

Egelman, E. H. 1985. The structure of F-actin. *J. Muscle Res. Cell Motil.* 6:129–151.

Funatsu, T., Y. Harada, M. Tokunaga, K. Saito, and T. Yanagida. 1995. Imaging of single fluorescent molecules and individual ATP turnovers by single myosin molecules in aqueous solution. *Nature.* 374:555–559.

Güttler, F., J. Sepiol, T. Irngartinger, T. Plakhotnik, A. Renn, and U. P. Wild. 1994. Fluorescence microscopy of single molecules. *Chem. Phys. Lett.* 217:393–397.

Hirschfeld, T. 1976. Optical microscopic observation of single small molecules. *Appl. Opt.* 15:2965–2966.

Houk, T. W., Jr., and K. Ue. 1974. The measurement of actin concentration in solution: a comparison of methods. *Anal. Biochem.* 62:66–74.

Ishikawa, M., K. Hirano, T. Hayakawa, S. Hosoi, and S. Brenner. 1994. Single-molecule detection by laser-induced fluorescence technique with a position-sensitive photon-counting apparatus. *Jpn. J. Appl. Phys.* 33: 1571–1576.

Kinosita, K., Jr., H. Itoh, S. Ishiwata, K. Hirano, T. Nishizaka, and T. Hayakawa. 1991. Dual-view microscopy with a single camera: real-time imaging of molecular orientations and calcium. *J. Cell Biol.* 115:67–73.

Kron, S. J., and J. A. Spudich. 1986. Fluorescent actin filaments move on myosin fixed to a glass surface. *Proc. Natl. Acad. Sci. USA.* 83: 6272–6276.

Miyata, H., H. Hakozaki, H. Yoshikawa, N. Suzuki, K. Kinosita, Jr., T. Nishizaka, and S. Ishiwata. 1994. Stepwise motion of an actin filament over a small number of heavy meromyosin molecules is revealed in an *in vitro* motility assay. *J. Biochem.* 115:644–647.

Miyata, H., H. Yoshikawa, H. Hakozaki, N. Suzuki, T. Furuno, A. Ikegami, K. Kinosita, Jr., T. Nishizaka, and S. Ishiwata. 1995. Mechanical measurements of single actomyosin motor force. *Biophys. J.* 68:286–290.

Morikawa, K., and M. Yanagida. 1981. Visualization of individual DNA molecules in solution by light microscopy: DAPI staining method. *J. Biochem.* 89:693–696.

Ohichi, T., T. Hozumi, and S. Higashi-Fujime. 1993. In vitro motility of proteolytically cleaved myosin subfragment 1 on a lysine-coated surface. *J. Biochem.* 114:299–302.

Shera, E. B., N. K. Seitzinger, L. M. Davis, R. A. Keller, and S. A. Soper. 1990. Detection of single fluorescent molecules. *Chem. Phys. Lett.* 174:553–557.

Suzuki, K., Y. Tanaka, Y. Nakajima, K. Hirano, H. Itoh, H. Miyata, T. Hayakawa, and K. Kinosita, Jr. 1995. Spatiotemporal relationships among early events of fertilization in sea urchin eggs revealed by multiview microscopy. *Biophys. J.* 68:739–748.

Tait, J. F., and C. Frieden. 1982. Polymerization-induced changes in the fluorescence of actin labeled with iodoacetamidotetramethylrhodamine. *Arch. Biochem. Biophys.* 216:133–141.

Yanagida, T., M. Nakase, K. Nishiyama, and F. Oosawa. 1984. Direct observation of motion of single F-actin filaments in the presence of myosin. *Nature.* 307:58–60.